Biochemistry and Biophysics Reports 11 (2017) 191–197

Contents lists available at ScienceDirect

Biochemistry and Biophysics Reports

journal homepage: www.elsevier.com/locate/bbrep

Cyclic mechanical stretch contributes to network development of osteocyte-like cells with morphological change and autophagy promotion but without preferential cell alignment in rat

Nao Inaba, Shinichiro Kuroshima*, Yusuke Uto, Muneteru Sasaki, Takashi Sawase

Department of Applied Prosthodontics, Graduate School of Biomedical Sciences, Nagasaki University, 1-7-1, Sakamoto, Nagasaki-city, Nagasaki 852-8588, Japan

ARTICLE INFO

Keywords:
Mechanical stimulation
Autophagy
Osteocyte-like cells
Cell morphology
Preferential cell alignment
Apoptosis

ABSTRACT

Osteocytes play important roles in controlling bone quality as well as preferential alignment of biological apatite *c*-axis/collagen fibers. However, the relationship between osteocytes and mechanical stress remains unclear due to the difficulty of three-dimensional (3D) culture of osteocytes *in vitro*. The aim of this study was to investigate the effect of cyclic mechanical stretch on 3D-cultured osteocyte-like cells. Osteocyte-like cells were established using rat calvarial osteoblasts cultured in a 3D culture system. Cyclic mechanical stretch (8% amplitude at a rate of 2 cycles min^{-1}) was applied for 24, 48 and 96 consecutive hours. Morphology, cell number and preferential cell alignment were evaluated. Apoptosis- and autophagy-related gene expression levels were measured using quantitative PCR. 3D-cultured osteoblasts became osteocyte-like cells that expressed osteocyte-specific genes such as *Dmp1*, *Cx43*, *Sost*, *Fgf23* and *RANKL*, with morphological changes similar to osteocytes. Cell number was significantly decreased in a time-dependent manner under non-loaded conditions, whereas cyclic mechanical stretch significantly prevented decreased cell numbers with increased expression of anti-apoptosis-related genes. Moreover, cyclic mechanical stretch significantly decreased cell size and ellipticity with increased expression of autophagy-related genes, *LC3b* and *atg7*. Interestingly, preferential cell alignment did not occur, irrespective of mechanical stretch. These findings suggest that an anti-apoptotic effect contributes to network development of osteocyte-like cells under loaded condition. Spherical change of osteocyte-like cells induced by mechanical stretch may be associated with autophagy upregulation. Preferential alignment of osteocytes induced by mechanical load *in vivo* may be partially predetermined before osteoblasts differentiate into osteocytes and embed into bone matrix.

1. Introduction

Bone quality, which has been defined as “the sum of all characteristics of bone that influence the resistance to bone fracture [1],” is completely independent of bone mineral density (BMD). Bone quality plays a crucial role in determining bone strength with BMD. Particularly, both preferential alignment of biological apatite (BAp) *c*-axis/collagen fibers and osteocytes are key factors affecting bone quality [2]. Osteocytes, which reside within lacunae of bone matrix, play a central role in controlling bone quantity (bone volume). Mechanical load, in particular, is considered to be one of the essential factors regulating bone quantity, as mechanical unloading results in load-associated osteoporosis [3]. Mechanical load on bone tissue is converted to various mechanical stimuli such as fluid shear stress, hydrostatic pressure and direct deformation of osteocytes [4]. Recently, we reported that cyclic mechanical load on bone tissue via dental implants led to the development of osteocyte networks with preferential alignment of BAp *c*-axis/collagen fibers and increased bone volume around dental implants [5]. Moreover, it has been reported that preferential alignment of osteocytes occurred in response to mechanical stimulation [6]. However, when preferential alignment of osteocytes occurs, how osteocytes control bone quality and why osteocyte networks are improved in response to mechanical load remain unclear.

Autophagy and apoptosis, which are two distinct self-destructive processes, play an important role in degradation of cytoplasmic organelles and cell death, respectively. Autophagy is an intracellular degradation system that delivers cytoplasmic degraded components to lysosomes fused to autophagosomes [7]. Apoptosis is one of several types of programmed cell death that occurs by altering the balance between apoptosis-related proteins and anti-apoptosis-related proteins.

* Corresponding author.
E-mail addresses: bb55313205@ms.nagasaki-u.ac.jp (N. Inaba), kuroshima@nagasaki-u.ac.jp (S. Kuroshima), y-uto@nagasaki-u.ac.jp (Y. Uto), m-sasaki@nagasaki-u.ac.jp (M. Sasaki), sawase@nagasaki-u.ac.jp (T. Sawase).

http://dx.doi.org/10.1016/j.bbrep.2017.04.018
Received 22 January 2017; Received in revised form 21 April 2017; Accepted 26 April 2017
Available online 11 May 2017

Upregulation and downregulation of autophagy or apoptosis are influenced by multiple factors such as physiological stress, hormonal stimulation, drug exposure, bacterial infections, innate immune signals, senescence and several types of diseases including cancers and immune diseases [8,9]. Recently, it has been reported that both autophagy and apoptosis are also influenced by mechanical stress in mammalian cells [10]. However, the effect of mechanical stimulation on autophagy and apoptosis in osteocytes has not been investigated due to the difficulty in monitoring osteocytes *in vitro*. Here, we developed a three-dimensional (3D) culture system in which rat calvarial osteoblasts were differentiated into osteocyte-like cells *in vitro*. The aim of this study was to investigate the effect of cyclic mechanical stretch on cultured osteocyte-like cells in rat.

2. Materials and methods

2.1. Establishment of osteocyte-like cells derived from rat calvarial osteoblasts in a 3D culture system

Three female Wistar rats (12-week-old) were purchased (Biotek Co. Ltd., Saga, Japan). Calvarial osteoblasts were isolated as previously described [11]. To establish osteocyte-like cells *in vitro*, a 3D culture system was developed with modification of previous studies [12,13]. A silicone chamber (STREX Inc., Osaka, Japan) was coated with collagen type I rat tail (Corning, Inc., NY, USA) and 0.02 N acetic acid (Wako Pure Chemical Industries, Ltd., Osaka, Japan). Gel constructs were made using a 1:1 ratio of Matrigel (BD Biosciences, NJ, USA) and a collagen solution consisting of 58% collagen type I tail, 26% 5× DMEM, 2.5% FBS, 2.5% fetal calf serum (Gibco by Life Technologies, CA, USA), 0.05 N sodium hydroxide (Wako Pure Chemical Industries, Ltd.) and a 5% cell suspension (1×10^6 cells/mL). The gel was transferred to the collagen-coated silicon chamber and incubated at 37 °C for 60 min. Osteoblasts were cultured in this 3D culture system to facilitate network formation with cell process-like structures. Osteoblasts cultured on collagen type I rat tail and 0.02 N acetic acid coated-silicon chambers were used as control (designated as 2D culture). All experiments were performed in accordance with the guidelines for the Animal Experimentation of Nagasaki University, and the current protocol was approved by the Ethics Committee for Animal Research of Nagasaki University.

2.2. Mechanical stimulation of osteocyte-like cells in vitro

A loading device (ST-140, STREX Inc.) was used for mechanical stimulation. Silicon chambers were directly connected to the loading device. Cyclic mechanical stimulation was then initiated 24 hours after the start of 3D culture. Cells were cultured under continuous cyclic stretch of 8% amplitude at a rate of 2 cycles min^{-1}. Cyclic stretch amplitude > 8% was not used because the gel could not maintain its structure without tearing. Cyclic mechanical stimulation was applied for 24, 48 and 96 hours with medium changes every 2 days (Fig. 1A–D).

2.3. Fluorescent staining and quantitative morphological analyses

Cells were fixed with culture gel and stained for phalloidin A (Cytoskeleton Inc., Denver, CO, USA) and DAPI (TAKARA Bio Inc., Tokyo, Japan) for 30 minutes at 37 °C. Fluorescent microscopy (BZ9000, Keyence, Osaka, Japan) and CellProfiler software (Broad Institute, Cambridge, MA, USA) were used to visualize cells and for morphological analyses [14]. The images at half thickness from the bottom area were used for all analyses. Cell number, cell area, cell perimeter, major axis length, minor axis length, cell eccentricity, cell solidity and cell orientation were automatically measured using CellProfiler. Each parameter was determined as follows: (1) cell number and area (pixel) = the actual number of pixels in the region; (2) cell perimeter (pixel) = the total number of pixels around the boundary of each region in the image; (3) cell eccentricity = the eccentricity of the ellipse that has the same second-moments as the region. Eccentricity is the ratio of the distance between the foci of the ellipse and its major axis length; (4) major axis length (pixel) = the length of the major axis of the ellipse that has the same normalized second central moments as the region; (5) minor axis of length (pixel) = the length of the minor axis of the ellipse that has the same normalized second central moments as the region; (6) cell solidity (ratio) = the proportion of pixels in the convex hull that are also in the object; and (7) cell orientation (degree) = the angle between the x-axis and the major axis of the ellipse that has the same second-moments as the region. Absolute values of the cell alignment angle were used in this study.

2.4. Quantitative real-time polymerase chain reaction (qPCR)

Total RNA was extracted using TRIZOL (Invitrogen, CA, USA) and the phenol/chloroform method [15]. First strand cDNA was synthesized using the Promega system (Promega, WI, USA). Quantitative real-time PCR (qPCR) was conducted using the Thermal Cycler Dice system (TAKARA, Shiga, Japan) with SYBR green (Invitrogen). Samples were run in triplicate. All results were normalized to *β-actin* expression. Relative quantification of data generated using this system was performed using the standard curve method. The following primer sets were used: osteoblast-specific genes (*Runx2* and *Opn*), osteocyte-specific genes (*Cx43*, *E11*, *Mepe*, *RANKL*, *Dmp1*, *Fgf23* and *Sost*), apoptosis-related genes (*Bcl-XL*, *Bcl2*, *Bim*, *Bid*, *Bak1*, *Bax*, *PUMA*, *Casp3* and *Casp7*) and autophagy-related genes (*Ulk1*, *LC3b*, *Becn1*, *AMPKα1*, *AMPKα2*, *Mtor*, *p62/sqstm1*, *p62*, *atg7* and *p53*) (Table 1).

2.5. Statistics

Statistical analyses were conducted in a blinded manner. The Shapiro-Wilk test was performed to test for normality. The independent *t*-test and one-way analysis of variance were used for parametric data. The Kruskal-Wallis test was used for non-parametric data. All statistical analyses were conducted using SYSTAT 12 (Systat Software, Chicago, IL, USA). An α-level of 0.05 was used for statistical significance. All data are represented as the mean ± SEM.

3. Results

3.1. Effect of 3D culture for 120 hours on rat calvarial osteoblasts

Representative fluorescent images of 2D and 3D culture are shown in Fig. 2A. 2D- and 3D-cultured cells exhibited distinct morphology. 3D-cultured cells appeared to have cell process-like structures that connected to adjacent cells. *Runx2* expression was similar between 2D- and 3D- cultured cells (Fig. 2B). *OPN* expression in 3D-cultured cells was significantly higher than that in 2D-cultured cells (Fig. 2C). *Mepe* and *E11* expression levels were almost the same between 2D- and 3D-cultured cells (Fig. 2D, E), whereas *Dmp1*, *Cx43*, *Sost*, *Fgf23* and *RANKL* expression levels in 3D-cultured cells were significantly increased compared with those in 2D-cultured cells (Fig. 2F–J).

3.2. The effect of cyclic mechanical stretch on cell number and apoptosis

Cell numbers under loaded conditions at 96 hours after mechanical stretch appeared to be increased compared to that under non-loaded conditions (Fig. 3A, B). Cell number under non-loaded conditions was significantly decreased in a time-dependent manner, whereas it was not decreased at 48 and 96 hours after cyclic mechanical stretch (Fig. 3C). Cyclic mechanical stimulation significantly suppressed *Casp3* expression (Fig. 3D), whereas *Casp7* expression did not significantly change (Fig. 3E). Cyclic mechanical stimulation significantly increased *Bcl-XL* expression (Fig. 3F). *Bcl2* expression did not change, regardless of mechanical stimulation (Fig. 3G). Additionally, cyclic mechanical

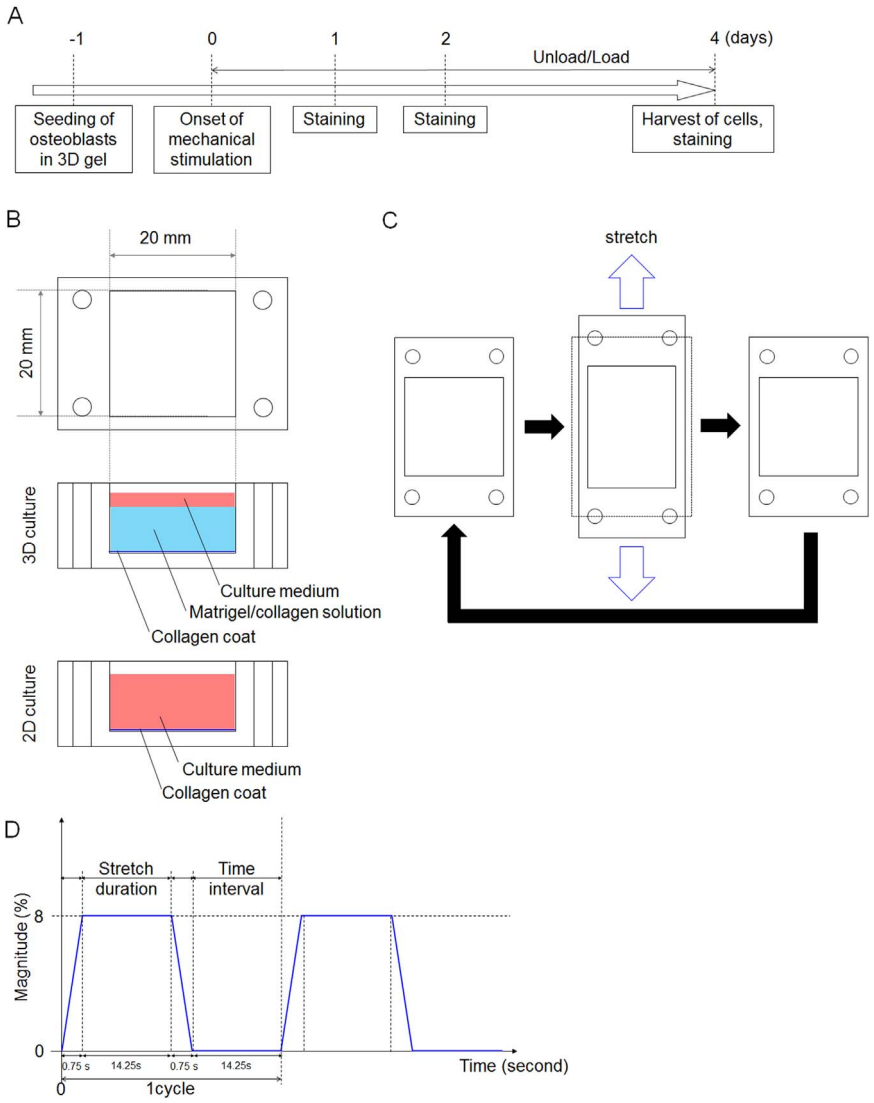

Fig. 1. Experimental design. (A) Mechanical stimulation was started at 24 hours after seeding of osteoblasts. (B) Culture system used in this study. A Matrigel/collagen solution was used for the 3D culture system. Collagen alone was used for the 2D culture system. (C) Schematic illustration of the silicone chamber and cyclic mechanical stimulation. The dotted line indicates the shape of the culture chamber before stretching. (D) Schematic waveform of applied mechanical stimulation in this study. The waveform represents 8% amplitude and a rate of 2 cycles min^{-1}.

stimulation significantly decreased the *Bim/Bcl-XL* ratio (Fig. 3H). The ratios of *Bak1/Bcl-XL*, *Bax/Bcl-XL* and *PUMA/Bcl-XL* under loaded conditions were smaller than those under non-loaded conditions, although the differences were not significant (Fig. 3I–K). The *Bid/Bcl-XL* ratio was the same between groups (Fig. 3L).

3.3. Effect of cyclic mechanical stimulation on autophagy

Cyclic mechanical stimulation for 96 hours significantly increased *LC3b* and *atg7* expression levels (Fig. 4A, B). However, *p62*, *p62/spstm1*, *Ulk1*, *Mtor*, *AMPKα1*, *AMPKα2*, *p53* and *Becn1* expression levels were similar under loaded and non-loaded conditions (Fig. 4C-J).

3.4. Effect of cyclic mechanical stimulation on morphology and preferential alignment of osteocyte-like cells

Cell morphology under loaded conditions for 96 hours appeared smaller than that under non-loaded conditions (Fig. 5A). Cyclic mechanical stimulation significantly decreased the cell area, perimeter, eccentricity, major axis length and minor axis length (Fig. 5B–F). Additionally, cyclic mechanical stimulation significantly increased cell solidity (Fig. 5G). The angle (θ) between the x-axis and long axis of cells was also measured (Fig. 5H). Cell distributions at each angle was almost the same, regardless of cyclic mechanical stimulation (Fig. 5I).

4. Discussion

Osteocytes exist in a 3D environment, however, most *in vitro* studies have been performed in a 2D environment. MLO-Y4, a mouse osteocyte-like cell line characterized by cellular proliferation, dendrite processes and osteopontin and Cx43 expression, is the most widely used cell line to investigate osteocyte function. However, MLO-Y4 expresses undetectable levels of *Dmp1* and *Sost* [16], although osteocytes highly express these genes in 3D environment. Thus, understanding osteocyte function has been challenging even when using MLO-Y4 cells. Some groups have used osteocyte-like cells developed in a 3D culture system to overcome this problem [12,17,18]. A recent study indicated that the function of 2D-cultured osteocyte-like cells was quite distinct from that of 3D-cultured osteocyte-like cells *in vitro* [13], indicating that a 3D environment is required to evaluate the function of osteocyte-like cells in *in vitro* studies. In the current study, the morphology of 3D-cultured osteoblasts was markedly changed with cell process-like structures that

Table 1
Primer sets.

Gene	Forward	Reverse
β-actin	GTAGCCATCCAGGCTGTGTT	CCCTCATAGATGGGCACAGT
Runx2	CGACAGCCCCAACTTCCT	ACGGTAACCACGGTCCCAT
Opn	AGACCATGCAGAGAGCGAG	ACGTCTGCTTGTGTGCTGG
Cx43	CTTCCTGCTCATCCAGTGGT	GGACGTGAGAGGAAGCAGTC
E11	ACCCCAATAGAGATAACGCAGG	CCAGGGTCACTACAGCCAAG
Mepe	AGGCTGTGTCTGTTGGACTG	AAGTGGATGTTGCCTTGGTT
RANKL	CATCGGGTTCCCATAAAG	GAAGCAAATGTTGGCGTA
Dmp1	CGGCTGGTGGTCTCTCTAAG	CTGGACTGTGTGGTGTCTGC
Fgf23	TTGGATCGTATCACTTCAGC	TGCTTCGGTGACAGGTAG
Sost	GGCAAGCCTTCAAGAATGATGCCA	TGTACTCGGACACGTCTTTGGTGT
Bcl-XL	TGCGTGGAAAGCGTAGACAAGGA	AAGGCTCTAGGTGGTCATTCAGGT
Bcl2	TGGAAAGCGTAGACAAGGAGATGC	CAAGGCTCTAGGTGGTCATTCAGG
Bim	AAACGATTACCGAGAGGCGGAAGA	AATGCCTTCTCCATACCAGACGGA
Bid	ACGACAAGGCCATGCTGATA	AGGCACCCTCAGTCCATCTC
Bak1	GAGTTTGCGTAGAGACCCCATCCT	CCACAAATTGGCCCAACAGAACCA
Bax	TGCTACAGGGTTTCATCCAG	CCAGTTCATCGCCAATTCG
PUMA	CGGAGACAAGAAGAGCAACA	TAGTTGGGCTCCATTTCTGG
Casp3	AGAAATTCAAGGGACGGGTC	TGCGCGTACAGTTTCAGCA
Casp7	TACAAGATCCCGGTGGAAGCT	CTGGGTTCCTCCACGAATAATAG
LC3b	CATGCCGTCCGAGAAGACCT	GATGAGCCGGACATCTTCCACT
Ulk1	GCTGCTCTCTTCAGGCTTACAG	CCTGCTTCACAGTAGACGAAAG
Becn1(Atg6)	TTGGCCAATAAGATGGGTCTGAA	TGTCAGGGACTCCAGATACGAGTG
AMPKα2	TGGAGGTGAATTGTTCGACTACAT	ACAGTAGTCCACGGCAGACAGA
AMPKα1	TGTGGCTCGCCCAATTATG	GACCCCGCTGCTCCAGAT
Mtor	TGGAGGGAGAGCGTCTGAGA	TGATGTGCCGAGGCTTTGT
P62/sqstm1	CCATGGGTTTCTCGGATGAA	GGAGGGTGCTTGGAATACTGG
p62	GCTGCTCTCTTCAGGCTTACAG	CCTGCTTCACAGTAGACGAAAG
Atg7	CGATGGCTTCCTACTGTTATT	CATGACAACAAAGGTGTCAAA
p53	CATGAGCGTTGCTCTGATG	CAGATACTCAGCATACGGATTTCC

connected to adjacent cells compared with 2D-cultured osteoblasts. As expected, expression of *Dmp1*, *Cx43*, *Sost*, *Fgf23* and *RANKL*, but not *Mepe* and *E11*, which are recognized as osteocyte-specific genes, was significantly increased in 3D-cultured osteoblasts compared with 2D-cultured osteoblasts. An *in vitro* study using human osteocyte-like cells established from osteoblasts in a unique 3D culture system also examined osteoblast- and osteocyte-specific gene expression levels to evaluate whether osteoblasts grown in 3D culture could differentiate into osteocyte-like cells [12]. Hence, osteoblasts cultured for 120 hours in the 3D culture system were designated as osteocyte-like cells and used to investigate the effect of mechanical stimulation in this study.

Long-term cell culture in a 3D system under cyclic mechanical load is challenging. Too strong cyclic mechanical stretch can rupture gels containing cells, while too weak cyclic mechanical stretch does not induce cell responses. It has been reported that the threshold of stress amplitude was 4–8% for osteoblasts in a 2D culture system [19]. In this study, amplitude > 8% tore the gels within 2–3 days. Moreover, 3D-cultured cells indirectly received mechanical stimuli via gels, resulting in reduced stress amplitude transmitted to osteocyte-like cells. Hence, 8% stress amplitude was selected to compensate for cell responses to

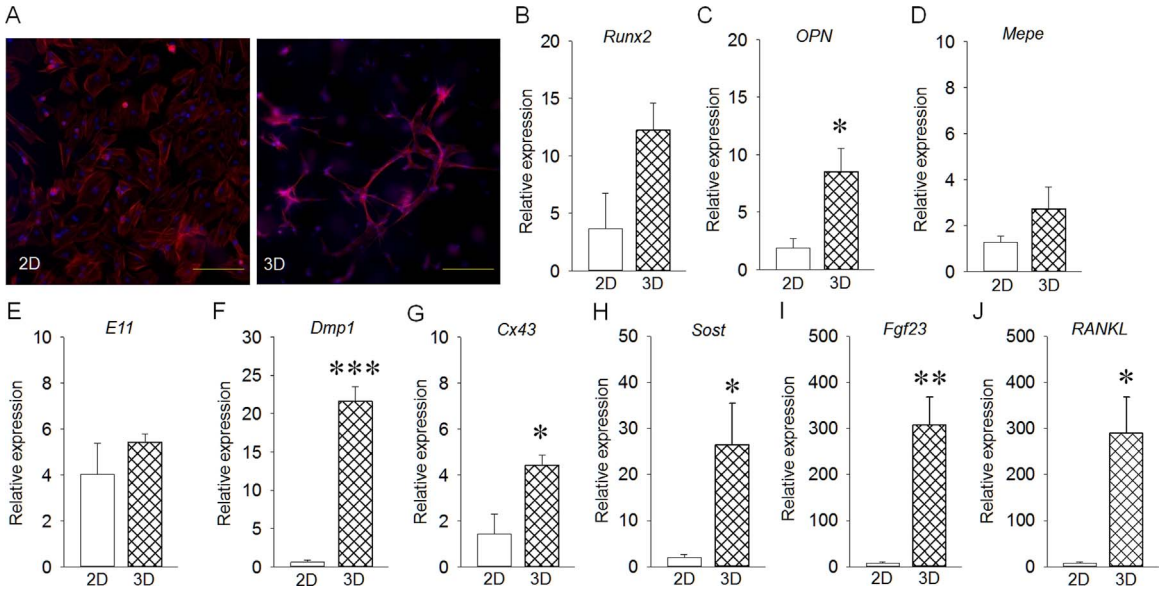

Fig. 2. Effect of 3D culture on rat calvarial osteoblasts for 120 hours *in vitro*. (A) Representative images for 2D- and 3D-cultured cells (Bar: 100 μm). (B) *Runx2* expression was similar in 2D- and 3D-cultured cells. (C) *OPN* expression in 3D-cultured cells was significantly increased compared with that in 2D-cultured cells. (D, E) Both *Mepe* and *E11* expression levels were the same between groups. (F–J) *Dmp1*, *Cx43*, *Sost*, *Fgf23* and *RANKL* expression levels in 3D-cultured cells were significantly increased compared with those in 2D-cultured cells. Results are expressed as relative gene expression after normalization to the house-keeping gene *β-actin*. $^{*}p < 0.05$, $^{**}p < 0.01$, $^{***}p < 0.001$.

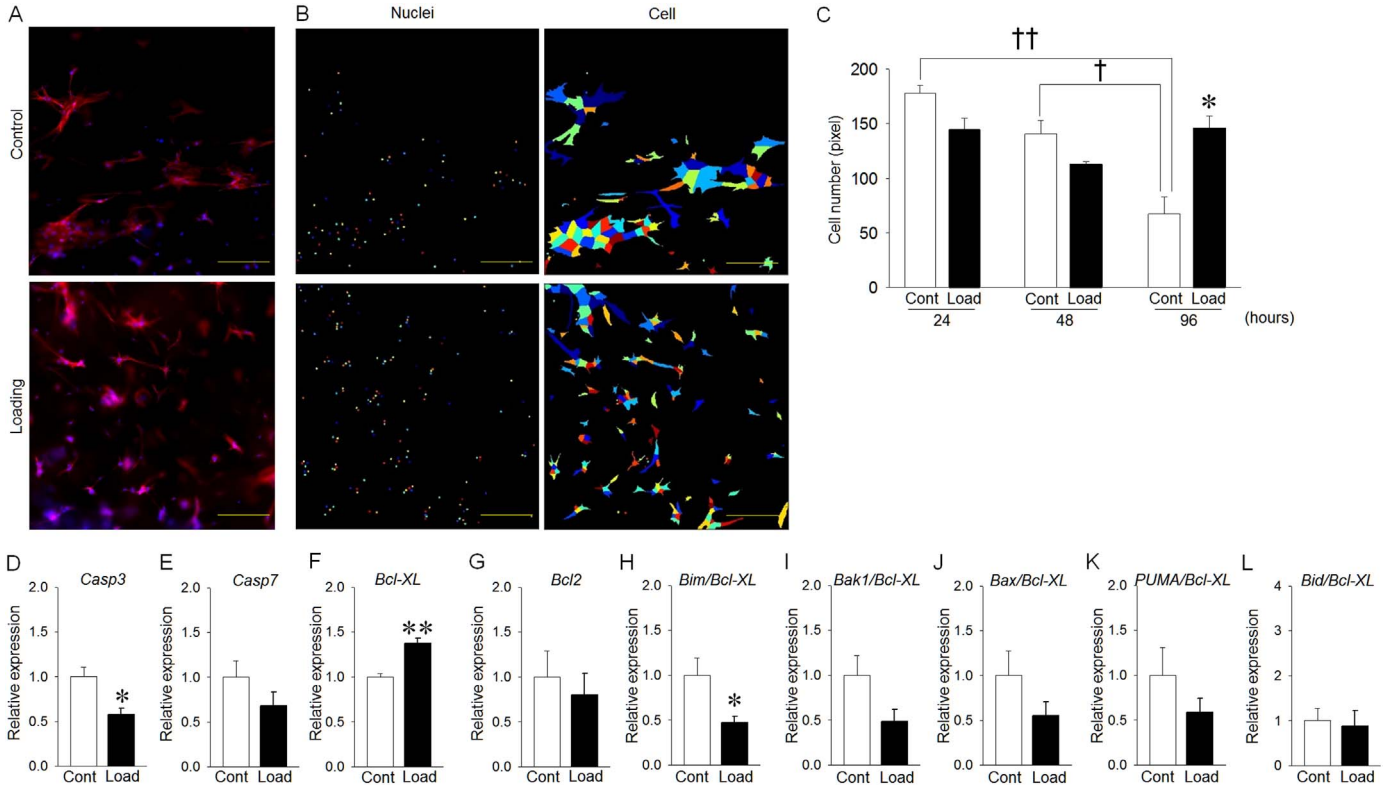

Fig. 3. Effect of mechanical stretch on cell number and apoptosis-related genes of osteocyte-like cells. (A) Representative fluorescent images at 96 hours after mechanical stretch (Bar: 100 μm). (B) Each color represents cell shapes and nuclei. (C) The cell number in the control group was significantly decreased in a time-dependent manner, whereas the cell number in the loading group was not significantly decreased. (D) *Casp3* expression in the loading group was significantly decreased compared with that in the control group. (E) *Casp7* expression was the same between groups. (F) *Bcl-XL* expression in the loading group was significantly increased compared with that in the control group. (G) *Bcl2* expression was the almost same between groups. (H) *Bim/Bcl-XL* expression in the loading group was significantly decreased compared with that in the control group. (I-K) *Bak1/Bcl-XL*, *Bax/Bcl-XL* and *PUMA/Bcl-XL* expression levels in the loading group were decreased compared with those in the control group, although the differences were not significant. (L) *Bid/Bcl-XL e*xpression was the same between the loading and control groups. Results are expressed as relative gene expression after normalization to the housekeeping gene *β-actin*. $*p < 0.05$, $**p < 0.01$, † $p < 0.05$, †† $p < 0.01$.

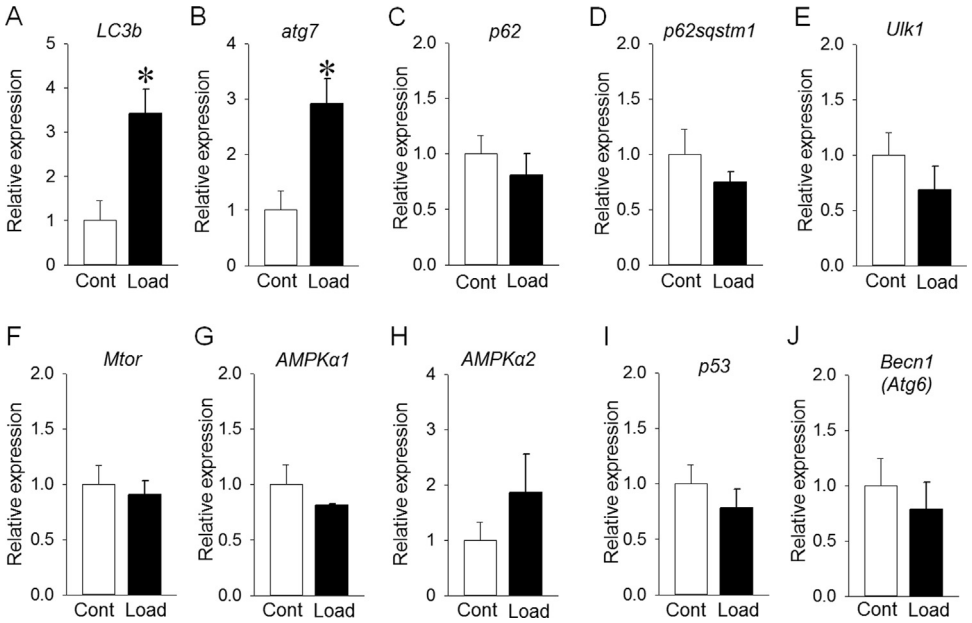

Fig. 4. Effect of mechanical stimulation for 96 hours on autophagy-related genes. (A) *LC3b* expression in the loading group was significantly increased compared with that in the control group. (B) *atg7* expression in the loading group was significantly increased compared with that in the control group. (C-J) *p62*, *p62sqstm1*, *ULK1*, *Mtor*, *AMPKα−1*, *AMPKα−2*, *p53* and *Becn1* expression levels were almost the same between the loading and control groups. Results are expressed as relative gene expression after normalization to the housekeeping gene *β-actin*. $*p < 0.05$.

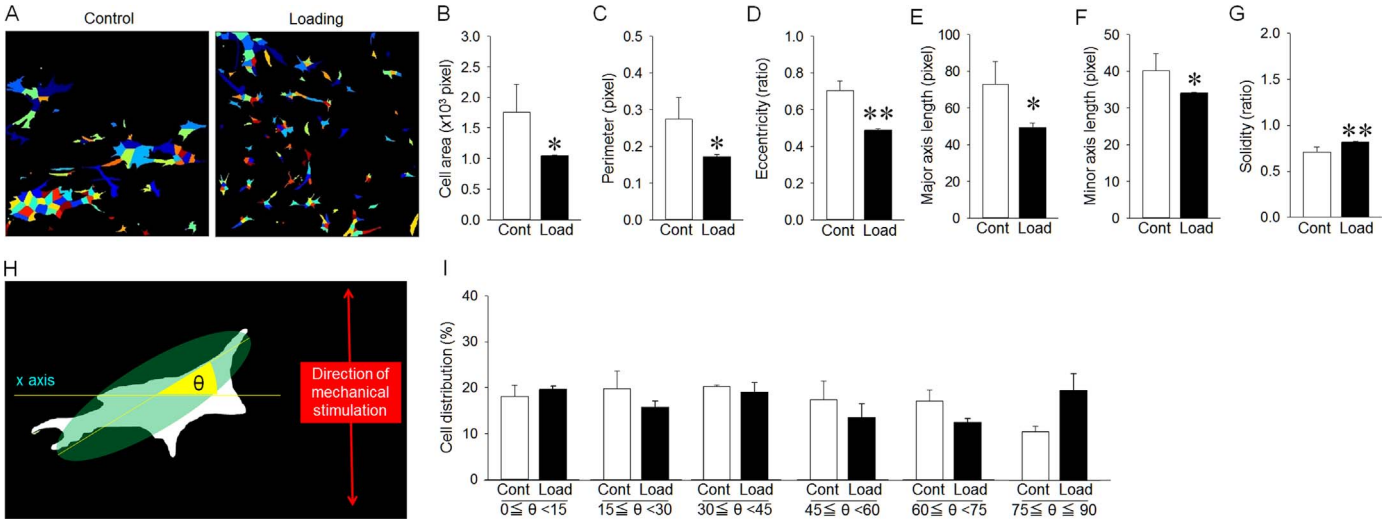

Fig. 5. Effect of mechanical stimulation for 96 hours on morphology and preferential alignment of cells *in vitro*. (A) Analyzed diagrams of cell outlines using CellProfiler software. Each color represents cell nuclei. (B) Cell area in the loading group was significantly smaller than that in the control group. (C) Cell perimeter in the loading group was significantly smaller than that in the control group. (D) Cell eccentricity in the loading group was significantly shorter than that in the control group. (E) Major axis length in the loading group was significantly shorter than that in the control group. (F) Minor axis length in the loading group was significantly smaller than that in the control group. (G) Cell solidity in the loading group was significantly larger than that in the control group. (H) Schematic illustration indicates cell alignment to the direction of mechanical stimulation. The x-axis was orthogonal to the direction of mechanical stimulation. The angle (θ) between the x-axis and long axis of cells was measured. (I) Cell orientation did not change between the loading and control groups, irrespective of the angle between the x-axis and long axis of cells. $*p < 0.05$, $**p < 0.01$.

cyclic mechanical stretch. Additionally, a rate of 2 cycles min^{-1} was applied according to a previous study that demonstrated preferential alignment of osteoblasts by cyclic mechanical stretch in a 2D culture system [14].

It has been demonstrated that mechanical unloading significantly reduced density of osteocyte lacunae compared with loading in rat tibiae [20], and osteocyte density in peri-implant bone under loaded conditions was significantly increased compared with non-loaded conditions in a human study [21]. Moreover, we demonstrated that cyclic mechanical load via dental implants significantly increased osteocyte density around the implant neck *in vivo* [5,22]. These findings suggest that the osteocyte network is upregulated by mechanical stimuli in both jaw and skeletal bones. However, clarification of the mechanisms by which mechanical stimuli alter osteocyte density have been challenging because many studies that examined osteocyte density were 2D-*in vitro* studies. Thus, we developed a 3D culture system to elucidate the mechanism. Cyclic mechanical stimulation significantly increased the number of osteocyte-like cells. This was in accordance with previous *in vivo* studies [20–22]. A recent study indicated that stretch force had an anti-apoptotic effect on 2D-cultured MLO-Y4 cells by suppressing caspase-3 activity and enhancing translocation of Src kinases [23]. In the current study, *Casp3* expression significantly decreased under mechanical load. Moreover, anti-apoptotic gene (*Bcl-XL* but not *Bcl2*) expression significantly increased, and the ratios of pro-apoptotic genes to *Bcl-XL*, especially *Bim/Bcl-XL*, were decreased. It has been suggested that cell phenotypes and force types influence the expression patterns of apoptotic- and anti-apoptotic-related genes [24]. For instance, high shear stress increases Bcl-XL production in endothelial cells [25], whereas mechanical stretch induces Bad and Bax production in cardiomyocytes, but not in fibroblasts [26]. Our findings suggest that mechanical stimulation could have an anti-apoptotic effect on 3D-cultured osteocyte-like cells. Osteocyte-like cells survived but did not increase under cyclic loaded conditions, indicating that development of osteocyte networks by mechanical stimulation may contribute to decreased apoptosis of osteocytes.

There are no reports that investigated the effect of mechanical stimuli on autophagy in osteocytes *in vitro* and *in vivo*. To our knowledge, this is the first *in vitro* study to demonstrate that cyclic mechanical stretch significantly increased *LC3b* and *atg7* expression levels with decreased cell area and ellipticity, indicating the shape of 3D-cultured osteocyte-like cells became spherical. Both LC3b and Atg7 are requisite for autophagosome formation [27]. *In vivo* studies have reported that a decline in autophagy-related gene *atg7* from osteocytes decreased bone mass with decreased osteoclast number, osteoblast number and bone formation rate. Moreover, *atg7* deletion in osteocytes significantly increased the diameter of mouse osteocytes and changed their shape [28,29]. Therefore, mechanical stimuli could trigger autophagy. Our findings also suggest that osteocyte-associated bone quality is controlled by changing the osteocyte network through changes in cell number, shape and size via expression of autophagy-related genes, especially *atg7*, in osteocytes under loaded conditions.

Preferential alignment of osteocytes has been demonstrated to be parallel to the direction of principal stress within the 60°-clockwise-grooves relative to a plane perpendicular to the long axis of hip implants in beagle dog [6]. Another study indicated that alignment of the long axis of osteocytes was parallel to the principal mechanical load direction in mouse fibulae, whereas osteocytes were randomly aligned in mouse calvariae [30]. Moreover, it has been demonstrated that osteocyte lacunae in human osteons are mainly located in longitudinally structured lamellae with an angle of 26–27° from the osteon axis which is parallel to the principal mechanical loading axis in long bones [31,32]. The shape of osteocyte lacunae corresponds with osteocyte shape in human long bones [33]. From these previous findings, preferential alignment of osteocytes is thought to range from parallel to approximately 30° to principal mechanical load directions in a site-specific manner. However, our present data were not consistent with these *in vivo* findings; our osteocyte-like cells did not have preferential alignment along the force direction under loaded conditions. Experimental conditions such as types of mechanical stimuli, animal species, differences between *in vivo* and *in vitro* cultures and observation methods would affect the preferential alignment of osteocyte-like cells. To our knowledge, there have been no *in vitro* studies investigating the relationship between osteocyte alignment and mechanical load.

In contrast, a previous report showed that specific cyclic stretch significantly induced preferential alignment of osteoblastic cell line MC3T3-E1 with approximately 60° of orientation angle to the principal load direction [34]. It has also been reported that cyclic mechanical stretch induced preferential alignment of 2D-cultured osteoblasts at

approximately 60° to the force direction *in vitro* [14]. The definitive reason why osteoblast alignment did not correspond with the force direction remains unclear. However, the authors concluded that elastic properties of poly-dimethylpolysiloxane, which was used as a cell culture substrate may be the cause of cell alignment at 60° to the principal mechanical load direction because the strain of poly-dimethylpolysiloxane was approximately 60° to the stretch direction. Accordingly, various factors including use of poly-dimethylpolysiloxane and thick gels may change principal mechanical load direction, resulting in the absence of the preferential alignment of osteocyte-like cells in this study.

Our current findings and previous data suggest that preferential alignment of osteocytes along the principal mechanical load direction is partially predetermined (e.g. approximately 60° to the principal force direction) before differentiation into osteocytes that embed into bone matrix. Osteocytes can access perilacunar calcium (osteocytic osteolysis) during periods of calcium depletion and synthesize new matrix upon calcium repletion [35], which suggests that preferential alignment and osteocytes shape are modified by various factors such as mechanical stimuli and osteocytic osteolysis.

In summary, cyclic mechanical stretch contributed to network development of osteocyte-like cells by anti-apoptotic effect. Cyclic mechanical stretch also changed the size and shape of osteocyte-like cells without preferential cell alignment via upregulation of *LC3b* and *atg7*. Our 3D culture system is a useful tool to determine the original function of osteocyte-like cells, although more *in vitro* studies that mimic *in vivo* 3D environment are required. Both osteoblasts and osteocytes may be key regulators controlling bone quality when mechanical stimuli are applied to bone tissue.

Acknowledgements

This work was supported by JSPS KAKENHI Grant Number 25670824.

Appendix A. Transparency document

Supplementary data associated with this article can be found in the online version at http://dx.doi.org/10.1016/j.bbrep.2017.04.018.

References

[1] D.P. Fyhrie, Summary–measuring "bone quality", J. Musculoskelet. Neuron. Interact. 5 (2005) 318–320.
[2] T. Nakano, K. Kaibara, Y. Tabata, N. Nagata, S. Enomoto, E. Marukawa, Y. Umakoshi, Unique alignment and texture of biological apatite crystallites in typical calcified tissues analyzed by microbeam X-ray diffractometer system, Bone 31 (2002) 479–487.
[3] D.D. Bikle, B.P. Halloran, The response of bone to unloading, J. Bone Miner. Metab. 17 (1999) 233–244.
[4] J. Klein-Nulend, A.D. Bakker, R.G. Bacabac, A. Vatsa, S. Weinbaum, Mechanosensation and transduction in osteocytes, Bone 54 (2013) 182–190.
[5] S. Kuroshima, T. Nakano, T. Ishimoto, M. Sasaki, M. Inoue, M. Yasutake, T. Sawase, Optimally oriented grooves on dental implants improve bone quality around implants under repetitive mechanical loading, Acta Biomater. (2016).
[6] Y. Noyama, T. Nakano, T. Ishimoto, T. Sakai, H. Yoshikawa, Design and optimization of the oriented groove on the hip implant surface to promote bone microstructure integrity, Bone 52 (2013) 659–667.
[7] N. Mizushima, B. Levine, A.M. Cuervo, D.J. Klionsky, Autophagy fights disease through cellular self-digestion, Nature 451 (2008) 1069–1075.
[8] G. Mariño, M. Niso-Santano, E.H. Baehrecke, G. Kroemer, Self-consumption: the interplay of autophagy and apoptosis, Nat. Rev. Mol. Cell Biol. 15 (2014) 81–94.
[9] N. Mizushima, T. Yoshimori, B. Levine, Methods in mammalian autophagy research, Cell 140 (2010) 313–326.
[10] J.S. King, D.M. Veltman, R.H. Insall, The induction of autophagy by mechanical stress, Autophagy 7 (2011) 1490–1499.
[11] S.E. Taylor, M. Shah, I.R. Orriss, Generation of rodent and human osteoblasts, Bone. Rep. 3 (2014) 585.
[12] F. Boukhechba, T. Balaguer, J.F. Michiels, K. Ackermann, D. Quincey, J.M. Bouler, W. Pyerin, G.F. Carle, N. Rochet, Human primary osteocyte differentiation in a 3D culture system, J. Bone Miner. Res 24 (2009) 1927–1935.
[13] L.E. Mulcahy, D. Taylor, T.C. Lee, G.P. Duffy, RANKL and OPG activity is regulated by injury size in networks of osteocyte-like cells, Bone 48 (2011) 182–188.
[14] A. Matsugaki, N. Fujiwara, T. Nakano, Continuous cyclic stretch induces osteoblast alignment and formation of anisotropic collagen fiber matrix, Acta Biomater. 9 (2013) 7227–7235.
[15] S. Kuroshima, Z. Al-Salihi, J. Yamashita, Mouse anti-RANKL antibody delays oral wound healing and increases TRAP-positive mononuclear cells in bone marrow, Clin. Oral. Investig. 20 (2016) 727–736.
[16] W. Yang, M.A. Harris, J.G. Heinrich, D. Guo, L.F. Bonewald, S.E. Harris, Gene expression signatures of a fibroblastoid preosteoblast and cuboidal osteoblast cell model compared to the MLO-Y4 osteocyte cell model, Bone 44 (2009) 32–45.
[17] J.M. Spatz, M.N. Wein, J.H. Gooi, Y. Qu, J.L. Garr, S. Liu, K.J. Barry, Y. Uda, F. Lai, C. Dedic, M. Balcells-Camps, H.M. Kronenberg, P. Babij, P.D. Pajevic, The Wnt inhibitor sclerostin is up-regulated by mechanical unloading in osteocytes in vitro, J. Biol. Chem. 290 (2015) 16744–16758.
[18] K. Uchihashi, S. Aoki, A. Matsunobu, S. Toda, Osteoblast migration into type I collagen gel and differentiation to osteocyte-like cells within a self-produced mineralized matrix: a novel system for analyzing differentiation from osteoblast to osteocyte, Bone 52 (2013) 102–110.
[19] C. Neidlinger-Wilke, E.S. Grood, J.H.-C. Wang, R.A. Brand, L. Claes, Cell alignment is induced by cyclic changes in cell length: studies of cells grown in cyclically stretched substrates, J. Orthop. Res. 19 (2001) 286–293.
[20] H.M. Britz, Y. Carter, J. Jokihaara, O.V. Leppänen, T.L. Järvinen, G. Belev, D.M. Cooper, Prolonged unloading in growing rats reduces cortical osteocyte lacunar density and volume in the distal tibia, Bone 51 (2012) 913–919.
[21] R.R. Barros, M. Degidi, A.B. Novaes, A. Piattelli, J.A. Shibli, G. Iezzi, Osteocyte density in the peri-implant bone of immediately loaded and submerged dental implants, J. Periodontol. 80 (2009) 499–504.
[22] M. Sasaki, S. Kuroshima, Y. Aoki, N. Inaba, T. Sawase, Ultrastructural alterations of osteocyte morphology via loaded implants in rabbit tibiae, J. Biomech. 48 (2015) 4130–4141.
[23] L.I. Plotkin, I. Mathov, J.I. Aguirre, A.M. Parfitt, S.C. Manolagas, T. Bellido, Mechanical stimulation prevents osteocyte apoptosis: requirement of integrins, Src kinases, and ERKs, Am. J. Physiol. Cell Physiol. 289 (2005) C633–643.
[24] D.D. Chan, W.S. Van Dyke, M. Bahls, S.D. Connell, P. Critser, J.E. Kelleher, M.A. Kramer, S.M. Pearce, S. Sharma, C.P. Neu, Mechanostasis in apoptosis and medicine, Prog. Biophys. Mol. Biol. 106 (2011) 517–524.
[25] B. Bartling, H. Tostlebe, D. Darmer, J. Holtz, R.E. Silber, H. Morawietz, Shear stress-dependent expression of apoptosis-regulating genes in endothelial cells, Biochem. Biophys. Res. Commun. 278 (2000) 740–746.
[26] X.D. Liao, X.H. Wang, H.J. Jin, L.Y. Chen, Q. Chen, Mechanical stretch induces mitochondria-dependent apoptosis in neonatal rat cardiomyocytes and G2/M accumulation in cardiac fibroblasts, Cell Res. 14 (2004) 16–26.
[27] M. Komatsu, S. Waguri, T. Ueno, J. Iwata, S. Murata, I. Tanida, J. Ezaki, N. Mizushima, Y. Ohsumi, Y. Uchiyama, E. Kominami, K. Tanaka, T. Chiba, Impairment of starvation-induced and constitutive autophagy in Atg7-deficient mice, J. Cell Biol. 169 (2005) 425–434.
[28] M. Piemontese, M. Onal, J. Xiong, L. Han, J.D. Thostenson, M. Almeida, C.A. O'Brien, Low bone mass and changes in the osteocyte network in mice lacking autophagy in the osteoblast lineage, Sci. Rep. 6 (2016) 24262.
[29] M. Onal, M. Piemontese, J. Xiong, Y. Wang, L. Han, S. Ye, M. Komatsu, M. Selig, R.S. Weinstein, H. Zhao, R.L. Jilka, M. Almeida, S.C. Manolagas, C.A. O'Brien, Suppression of autophagy in osteocytes mimics skeletal aging, J. Biol. Chem. 288 (2013) 17432–17440.
[30] A. Vatsa, R.G. Breuls, C.M. Semeins, P.L. Salmon, T.H. Smit, J. Klein-Nulend, Osteocyte morphology in fibula and calvaria — is there a role for mechanosensing? Bone 43 (2008) 452–458.
[31] G. Marotti, M.A. Muglia, D. Zaffe, A SEM study of osteocyte orientation inalternately structured osteons, Bone 6 (1985) 331–334.
[32] M. Petrtýl, J. Hert, P. Fiala, Spatial organization of the haversian bone in man, J. Biomech. 29 (1996) 161–169.
[33] G. Marotti, Osteocyte orientation in human lamellar bone and its relevance to the morphometry of periosteocytic lacunae, Metab. Bone Dis. Relat. Res 1 (1979) 325–333.
[34] K. Nagayama, Y. Kimura, N. Makino, T. Matsumoto, Strain waveform dependence of stress fiber reorientation in cyclically stretched osteoblastic cells: effects of viscoelastic compression of stress fibers, Am. J. Physiol. Cell Physiol. 302 (2012) C1469–1478.
[35] A. Teti, A. Zallone, Do osteocytes contribute to bone mineral homeostasis? Osteocytic osteolysis revisited, Bone 44 (2009) 11–16.